PAPER • **OPEN ACCESS**

Surface DBD plasma microbubble reactor for degrading methylene blue

To cite this article: Henrike Jakob *et al* 2023 *Phys. Scr.* **98** 025603

Physica Scripta

PAPER

Surface DBD plasma microbubble reactor for degrading methylene blue

Henrike Jakob[1], **Matthew Paliwoda**, **Joshua L Rovey**[2] and **Minkwan Kim**[1,*]

[1] Aeronautics and Astronautics Engineering Department, University of Southampton, Southampton, SO16 7QF, United Kingdom
[2] Aerospace Engineering Department, University of Illinois Urbana-Champaign, Urbana, IL, 61801, United States of America
* Author to whom any correspondence should be addressed.

E-mail: h.jakob@soton.ac.uk and m.k.kim@soton.ac.uk

Keywords: dielectric barrier discharge, non-thermal plasma, water treatment

OPEN ACCESS

RECEIVED
18 July 2022

REVISED
28 November 2022

ACCEPTED FOR PUBLICATION
20 December 2022

PUBLISHED
5 January 2023

Abstract

Water contaminants such as endocrine inhibitors, pharmaceuticals, and chlorine treatment by-products are only recently being identified as significant hazards to human health. Since current chlorine treatment does not address many of these compounds and conventional ozone processing is not seen as an economic alternative, water adjacent plasma treatment has been investigated as a more efficient and effective decontamination method. This work investigates the use of a surface dielectric barrier discharge electrode as a reduced discharge voltage portable plasma water treatment method. The gas passes through holes in the electrodes, normal to the discharge surface, so that the entire cross-sectional area of the feed gas is exposed to plasma, prior to passing through a hydrophobic filter and bubbling into the water. The decontamination effectiveness is quantified by measuring the degradation of methylene blue with absorption spectroscopy. Studies of the different processing parameters (treatment time, solution volume, initial concentration, electrode-filter distance, and gas flow rate) clarify the potential range of performance for this plasma treatment configuration. The setup has a yield energy of 0.45 g/kW·h at 25 ml of 1 mg/100 ml methylene blue treated over 5 minutes for a 92% degradation. The degradation rate is dependent upon the volume ratio of air to methylene blue solution, suggesting a first order chemical reaction process. The reaction rate is increased by increasing the quantity of either reactant. There is no change in the degradation between when the plasma is 1 mm or 1 cm from the water surface.

1. Introduction

Water pollutants from different industries have been shown to be able to pass through current chlorine water treatment systems without a reduction in concentration [1, 2]. Although the measured levels of pollutants are below allowable regulation limits, the build-up and long term effects of new or unregulated contaminants are a significant concern for public safety [3, 4]. For many of these pollutants, such as herbicides, pesticide, pharmaceuticals, and microplastics, there is limited control over their entry into drinking water sources. An alternative to the conventional chlorine treatment method, therefore, is required to secure drinking water safety from these contaminants.

Advanced oxidation processes (AOPs) are one alternative for removing water pollutants, and ozone based AOPs have gained growing attention due to its high oxidizing power and excellent disinfecting capabilities. Ozone has twice the oxidation potential of chlorine and one of the highest overall oxidation potentials, making it a more effective reagent than chlorine and able to address these new contaminants [5, 6]. Ozone and the free radical hydroxyl ($OH^{\bullet}$), which it produces in water, can decompose organic compounds [7]. The major advantages of ozone treatment are faster treatment time, more effective disinfectant, no harmful residuals, no chemical transportation and storage safety issues, and improved taste [6]. However, ozone is unstable, reducing to oxygen gas at a half-life rate ranging from seconds to a day, depending on the mass flow rate, humidity, and temperature [8]. For this reason it is manufactured at water treatment facilities by plasma discharge, which has

become a more prevalent method of water treatment [9]. Chlorine treatment is generally accepted as being more economical than ozone treatment [10], although this position has been disputed by the ozone water treatment community [11]. This has driven researchers towards improving the efficacy of the ozone treatment process.

Along with ozone, the plasma discharge produces free-radical species during the ionization process. The high electric field of the discharge accelerates electrons which collide into the working gas to break the molecular bonds and create the unstable species. The energy input of the discharge is effectively used to raise the bond potential of the gas species which then breaks the bonds of the water contaminants [12]. In conventional ozone AOPs, most of the free radicals are neutralized during transport from the discharge source to the water surface. This creates a loss mechanism as the discharge energy is reabsorbed within the chemical bonds. The goal of plasma water treatment compared to conventional ozone water treatment is to move the plasma source adjacent to the water. Plasma produced at the surface of the liquid allows transfer of reactive species that would otherwise recombine before reaching the liquid surface, introduces hydrogen as a reactive species in the discharge, and adds additional plasma-liquid dynamics that would otherwise not occur with a plasma produced at a distance [13].

A variety of discharge methods and configuration have been studied for plasma-water treatment of Methylene Blue (MB), the indicator dye used in this study: arc discharge [14–16], dielectric barrier discharge (DBD) [17–30], plasma jets [31], and microwave plasma generation [32, 33]. Oxygen gas is the preferential feed gas [19] since it promotes the production of ozone by 2–4 times that of air [6]. Although low concentrations of nitrogen gas may be beneficial to ozone production, high concentrations of NOx recombines the ozone back to oxygen gas.

The efficiency of different plasma treatment systems is typically measured by the yield energy Y_{energy}, given in g/kW·h. The yield energy is defined by the total MB mass treated per total treatment input energy as [28]:

$$Y_{energy} = \frac{\Delta C \cdot V}{P_{dis} \cdot \Delta t} \tag{1}$$

where ΔC is the change in concentration, V the volume, P the power and Δt the treatment time. From this equation, the yield is increased by decreasing either the discharge power or the reaction time. A larger yield energy, means, less energy, through a larger discharge power or extended treatment time, is required to achieve a change in MB concentration.

The total reaction time is governed by the first-order reaction rate equation [16, 22, 28], and dependent upon the concentration of the two reactants, the MB concentration (C_{MB}) and the reactive gas concentration (C_{gas}). The reaction rate constant (k) can vary for different initial temperatures [16], pH values [21], and conductivities [21].

$$\frac{\partial C_{MB}}{\partial t} = -kC_{gas}C_{MB} \tag{2}$$

The reaction rate will increase with the concentration of the reactants as the probability of the two reactants interacting increases. From equation (1), a decreased reaction rate will increase the yield energy. So, to increase the efficiency for a given concentration of MB, the concentration of reacting gas must be increased. This is equivalent to a larger gas-to-liquid ratio within the reactor. However, there is another consideration beyond the quantity of gas within the reactor: the mass transfer of gas through the gas-liquid interface. The reactor may still perform inefficiently if the quantity of gas entering the liquid is restricted, limiting the interaction with the MB.

The mass transfer rate (N) of gas into the liquid volume (V_L) is modeled by the Lewis-Whitman twin film model [34, 35].

$$N = (k_a a)(mC_G - C_L)V_L \tag{3}$$

The model assumes there is a gas-liquid interface made up of two thin layers of gas and liquid with decreasing gas concentrations, from the high concentration bulk gas to the low concentration bulk liquid. The liquid transfer coefficient (k_a) and solubility ratio (m) are intensive properties of the gas-liquid interface, independent of the plasma discharge configuration. The reactive species concentration (C_G) is dependent upon the discharge power that determines the plasma density and the plasma proximity to the surface since the species will recombine as they move from the plasma region to the liquid surface. The mass transfer rate decreases as the liquid concentration (C_L) increases until the liquid concentration reaches saturation. The area per unit of liquid volume (a) is dependent upon the configuration by which the gas interfaces with the liquid.

According to equation (3), to maximize the mass transfer of reactive species to a set liquid volume: the gas concentration is increased, the liquid concentration at the surface is reduced, or the area per unit liquid volume is increased. To increase efficiency, these three variables must be increased without requiring an increase in discharge power. The reactive species concentration of the gas can be increased by placing the plasma discharge adjacent to the liquid surface. The liquid concentration at the surface can be reduced by mixing the liquid. The mixing process replaces high concentration liquid at the gas-liquid interface with low concentration liquid. The

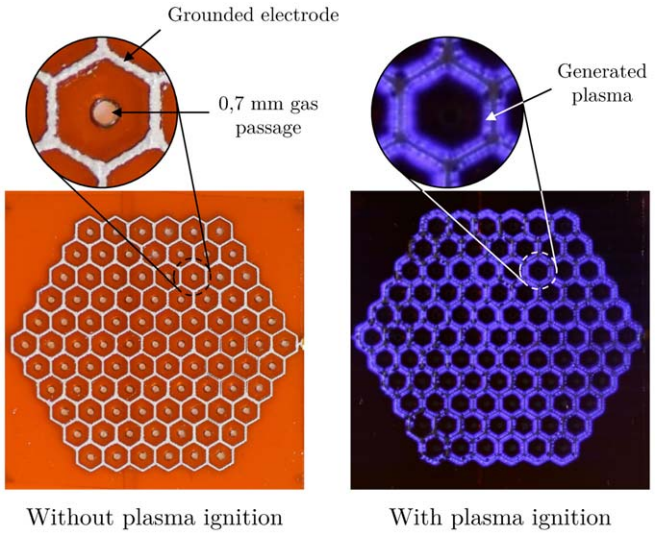

Figure 1. Porous surface DBD plasma generator.

area per unit liquid volume can be increased by increasing the volume ratio of gas-to-liquid. The surface area of the liquid per unit volume increases as the liquid volume decreases, due to the squared-to-cubic relationship of area-to-volume. Different two-phase flow regimes (bubble, slug, churn, surface flow, and misting) [36] can be implemented to reduce the volume ratio of gas to liquid.

So, a major variable for increasing efficiency, in both for the reaction rate and the mass transfer across the gas-liquid interface, is the increase of the gas-to-liquid ratio. As part of this work, we study the parameter space of a plasma discharge setup. To highlight the importance of the gas-to-liquid ratio, the changes to the different parameters are related back to a gas-liquid volume ratio.

Other researchers have already investigated the parameters of treatment time, gas flow rate, and MB concentration as they relate to the degradation rate and yield energy. The MB solution has an exponential degradation with treatment time, characteristic of a first-order chemical reaction [16, 22, 28]. Increased gas flow increases the degradation over a fixed time [20–22, 25, 32]. Garcia *et al* [32] found a linear increase between gas flow and the quantity of excited Argon atoms at the water surface, based on light intensity measurements. Wu *et al* [21] found that the ozone production also increased with air flow. However, there was an upper limit above 1.5 L/min which was assumed to be due to the limited energy provided by the reactor. Increased initial concentrations of MB decreases the degradation efficiency for a fixed treatment time [18, 21, 22, 28, 32]. Garcia *et al* [32] found the initial concentration to decrease the yield energy, hypothesizing that the additional intermediates from the degradation process competed with the MB decomposition. However, Krosuri *et al* [28] found the initial concentration to increase the yield energy, even with an increased reaction time. Although the reaction time approximately doubled, the treated MB mass increased by an order of magnitude. This was explained as an increase to the collision probability between the degrading gas species and the MB, in the higher MB concentration. Although these studies have investigated the trends of common parameters, the discussion of plasma water treatment efficiency can be furthered by relating the observed trends back to the governing principles of equation (2) and equation (3), through the gas-to-liquid ratio.

The discharge approach used in this study is a surface DBD, unique from previous volume DBD configurations. A volume DBD consists of a gas-gap separating two dielectric barrier covered electrodes, where a plasma is formed within the gas-gap. A surface DBD consist of two electrodes off-set along a separating dielectric barrier which creates a plasma on top of the surface of the barrier from the surrounding gas [37]. The benefit of the surface DBD is its reduced driving voltage and power requirement, due to the reduced discharge distance between the electrodes ($\sim$10 μm rather than $\sim$1 mm), requiring a lower breakdown voltage based off the Paschen curve relationship [38]. Figure 1 shows the developed porous surface DBD plasma source. The upper and lower electrodes are arranged in an overlapping hexagonal pattern with feed gas flowing through holes inside each hexagon, normal to the surface of the electrodes. This pattern serves to distribute the plasma over a large cross-sectional area of the feed gas. A hydrophobic membrane, separating the water and discharge cell, minimizes the plasma-water separation to bring the source of free-radicals within millimeters of the water surface without risking a short. The filter distributes bubbles over the membranes area to increase the gas-liquid surface area.

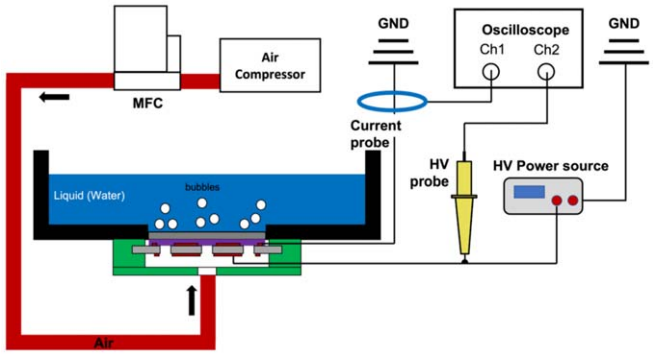

Figure 2. Schematic of experimental test setup.

This method is constructed for a small-scale portable water treatment system to process laboratory waste, making the reduced power system requirements more attractive. Using a small-scale portable water treatment system allows for a potential wider applicant of non-thermal plasma as a water treatment method. This study analyzes the parameter space—treatment time, gas flow rate, contaminant concentration, plasma-to-filter distance, and treatment volume—to optimize for the maximum degradation. Each parameter is equated to a air-water ratio to relate parameters effect on the degradation rate back to variables of equation (2). The yield energy is compared with other MB plasma treatment systems found in literature. The work is carried out as part of a collaborative project between the University of Southampton (UoS) and University of Illinois Urbana-Champaign (UIUC).

2. Material and methods

2.1. Plasma bubble reactor and porous surface DBD plasma generator

The experimental setup for the plasma microbubble generation consist of the plasma bubble reactor, the high voltage power supply system and the air supply system, schematically depicted in figure 2. The plasma bubble reactor has a fully sealed air intake enclosure that bubbles into a solution container, which are separated and sealed by a sandwich design of a porous surface DBD plasma source and a hydrophobic PTFE membrane of pore size 0.2 μm (Sartorius Hydrophobic PTFE Membrane Filters Type 11 807). Plasma is generated on the porous surface DBD plasma source in the region between plasma source and membrane. The inflowing air in the bottom enclosure forces reactive species generated in the plasma through the membrane and generates microbubbles, which bring the water into contact with the plasma. The formation and size of the generated microbubbles is mostly dependent on characteristics of the membrane, such as pore size or wettability of the material. As the same type of membrane is used for all presented experiments, no variation of formation and size of the microbubbles is analysed in the framework of this paper. Figure 1 shows a schematic of the porous surface DBD plasma generator. Both the high voltage and grounded electrode are printed on dielectric substrate (Kapton, 75 μm thick) using conductive ink (Conductor Flex-2 ink, Voltera). The printed electrodes are cured at 160 °C for 30 minutes to achieve full strength and conductivity. An orifice with a 0.7 mm diameter is drilled into the surface DBD plasma source to allow air to pass through normal to the surface.

The porous surface DBD plasma source is powered by a high voltage power supply constructed from the series arrangement of a sinusoidal waveform generator (AD9850 DDS Signal Generator), an audio power amplifier (Kemo M034N, 40 Watt), and two 1:100 turn ratio high voltage transformers (ET/UNI-05 from Express Transformers & Controls Ltd.). The sinusoidal signal is step-wise amplified through the audio amplifier and the high voltage transformer and reaches a maximum amplitude of the high voltage signal output ranges up to 4.5 kV. The frequency of the signal remains constant for this study at 6 kHz. The electrical characteristics of the porous plasma sources are monitored using a high voltage probe (UoS: P6015A, Tektronix/UIUC: PVM-5, North Star) for the applied voltage and a Rogowski coil (UoS: Model 6585, Pearson Electronics/UIUC: Model 4100, Pearson Electronics) for the current. The air supply system consists of a mass flow controller (MC-series, Alicat Scientific) providing an air flow rate ranging from 0 to 12 slpm.

The electrical characteristic of the the plasma reactor is quantified using measurement of voltage, V, and current, I, readings. Both signals follow a sinusoidal waveform, with discharge spikes on the current wave form. The discharge power, P_{dis}, of the plasma reactor is calculated as follows:

$$P_{dis} = \frac{1}{T}\int_0^T V(t) \cdot I(t)dt \tag{4}$$

from which the average discharge power, P_{ave}, is calculated by averaging the discharge power over the total number of sinusoidal periods, k, of the measured signal:

$$P_{ave} = \sum_{n=1}^{k} P_{dis} \tag{5}$$

In this study, the operating conditions for the plasma source are kept constant for the respective parameter studies. This results in a constant discharge power and assumed constant generation of reactive species. Within this study, the absolute generation of specific reactive species such as ozone is not analysed. The focus of this paper is placed upon the MB degradation efficiency effect from varying parameters of the plasma bubble reactor.

2.2. Material and sample preparation

In this study, we use methylene blue (MB) (3,7-bis (Dimethylamino)-phenothiazin-5-iumchloride) as an indicator of water pollutants removal efficiency because it is non-biodegradable and a common water pollutant found in most industrial wastewater [39]. MB is commonly used as a general dye and used for biological staining. MB has two distinct absorption peaks for quantitative spectroscopic measurement of the concentration [40] and a strong blue colour at 1mg/100 ml for visual qualitative inspection. Foster *et al* [31]. Measured MB concentrations for different plasma treatment times, using both absorption and chromatography. The agreement between the spectroscopic and direct mass measurements validates the use of absorption as a MB concentration measurement method during plasma degradation of the MB solution. The mass spectra in that work also showed few degradation intermediates until the MB solution was significantly degraded, suggesting a mineralization process. Reddy *et al* [22] demonstrated that the quantity of total organic carbon (TOC) in a MB solution decreased with plasma treatment, suggesting mineralization of the MB solution. Krosuri *et al* [28] measured the chemical oxygen demand (COD), sulphate, and chloride where the reactive gas was produced in a plasma at a distance from the water surface. The decrease of COD and increase of both sulphate and chloride suggested mineralization of the MB, even when the plasma is not in contact with the water surface. Absorption spectroscopy has extensively been used in literature [14–29, 31–33] to determine MB concentration and quantify its degradation during plasma-water treatment. The degradation of MB solution under plasma treatment will be analyzed in the same way for this work.

In this study the MB solution is prepared by dissolving MB powder (Scientific Laboratory Supplies Ltd. - CHE2582) in deionised water. The MB powder is weighed using an analytical weight balance (UoS: Kern, ABS 220/UIUC: Sartorius, Quintix 125D-1S) with a resolution of (UoS: ±0.1 mg/UIUC: ±0.001 mg) and the deionised water is measured in a volumetric flask with the tolerance of (UoS: ±0.4 ml/UIUC: ±2.5 ml). The baseline MB solution of 1 mg/100 ml is achieved by dissolving (UoS: 4 mg/UIUC: 5 mg) of MB into (UoS: 1 L/ UIUC: 500 ml) of deionised water to generate stock solution, which is then further diluted down to the final MB solution of 1 mg/100 ml (UoS: ±3%/UIUC: ±1%). Preparation of a high concentration stock solution results in lower error margin due to the larger relative error in the weight measurement of MB. Lower concentrations are achieved by mixing the baseline solution with deionised water.

2.3. Absorption Spectroscopy

The efficiency of the plasma microbubble treatment procedure is analysed by measuring the absorbance of treated MB solutions using absorption spectroscopy. The absorbance is measured using a spectroscopy setup (Ocean Optics, HR4000) at UoS and a photometer (Hanna instrument, HI-83300) at UIUC. The ocean optics spectroscopy setup consists of a halogen light source (Ocean Optics, DH-mini), a cuvette holder and the spectrometer with a wavelength range from 200 to 1100 nm (Ocean Optics, HR4000). The MB solution sample is filled in a plastic cuvette and placed in the cuvette holder, where the absorbance is measured over the full wavelength range. The photometer setup relies on the same principal, with an integrated light source at a fixed wavelength of 610 nm. The 610 nm wavelength is chosen for measurement because it corresponds to one of two strong and dominant MB peaks.

The absorbance measurements, A, can be converted to MB concentration, C, using the Beer–Lambert Law [41], as:

$$C = \frac{A}{\epsilon\, d} \tag{6}$$

where ϵ is the MB extinction coefficient at 610 nm with 37 418 $cm^{-1}M^{-1}$ [40, 42], and d the cuvette diameters of 10mm at UoS and 22 mm at UIUC. The extinction coefficient is obtained from a tabulated spectrum performed by Prahl using a HP spectrophotometer using a 1 cm quartz cuvette filled with a 10 μM solution of MB in Water

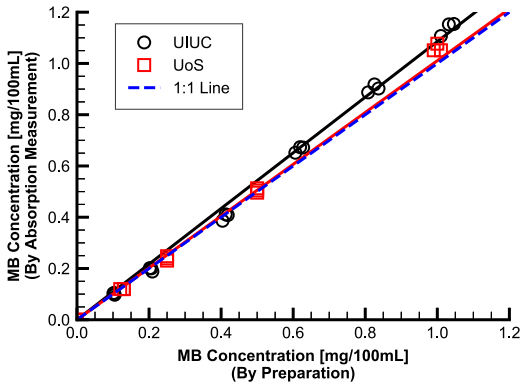

Figure 3. Concentration versus Concentration.

Table 1. Parameter variation

Parameters	Values	Group
Treatment time [min.]	1, 3, **5**, 7.5, 10	UoS, UIUC
Air flow rate [slpm]	0, 0.5, 1, **2**, 2.5, 3.5	UoS
Distance [mm]	0.9, 1.7, 2.5, 3.4, **4.5**, 1.9, 3.7, 6.5, 9.2, 12	UIUC
Concentration [mg/100ml]	0.1, 0.25, 0.5, 0.75, **1**	UoS
Treatment volume [ml]	15, **25**, 35, 40, 50	UIUC

[42]. This value agrees with published experimental and theoretical values reported by Fernandez-Perez and Gregorio Marban [40].

Absorption measurements at different prepared MB concentrations were performed to define three sources of MB absorption measurement error: agreement between UoS and UIUC data, initial sample preparation, and repeatability. The data sets are presented in figure 3 with curve-fits applied to both UoS and UIUC data sets that are forced to pass through the origin. A 1:1 unit line represents the ideal agreement between the absorption and prepared concentrations. Although the vials and test setups between UoS and UIUC are different, the UIUC trendline is only 7.4% greater than the UoS trendline. The percent error from the 1:1 line for UoS and UIUC are 1.6% and 8.6%, respectively. The five UoS data sets and three UIUC data sets have standard deviations of less than 3% and 6%, respectively. Although additional error is introduced by the experimental setups, the error values demonstrate the confidence in the solution preparation and measurement consistency.

Although the concentration calculation is necessary to validate the absorption measurement method, the remainder of this work reports the plasma processing capability in degradation efficiency, η, as a percent of the initial MB solution, defined by equation (7) [18, 19, 21, 22]. This approach is used to normalize the treated absorption, A_a, with the initial absorption, A_0, when evaluating the parameter variations.

$$\eta = \frac{A_0 - A_a}{A_0} \cdot 100 \tag{7}$$

2.4. Parameter study

The decontamination performance of the plasma microbubbles can be affected through various parameter: treatment time, air flow rate, distance between discharge electrode and water surface, initial MB concentration, and the treatment volume. The performance is evaluated in this study by measuring the percent degradation after 5 minutes of treatment, except for the time study which only evaluated the percent degradation for each time step. Table 1 lists the chosen parameters and the respective variation of the values along with a note of which group (UoS and/or UICC) carried out the respective test. For each parameter a baseline value (highlighted in bold font) is chosen, and were the values held fixed when the respective parameter was not being tested.

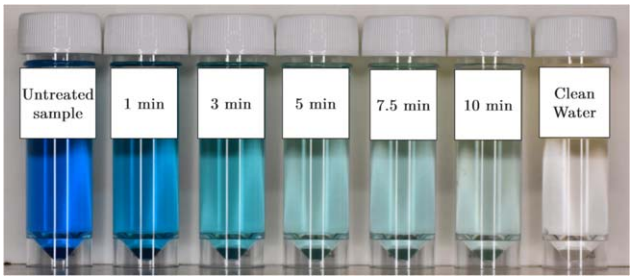

(a)

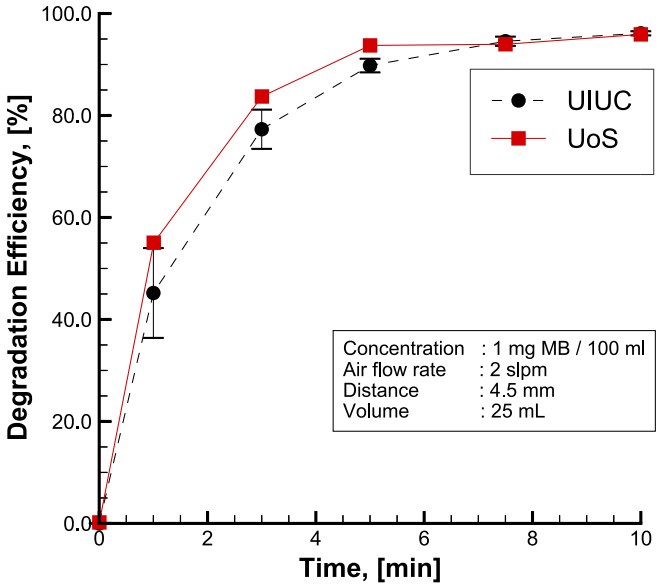

(b)

Figure 4. Effect of treatment time on degradation efficiency.

3. Results

3.1. Effect of treatment time

The degradation efficiency of a varying treatment time is analysed for times between 1 minute and 10 minutes. Figure 4(a) shows the MB solution in vials after each treatment time, compared with the untreated and clean water samples. As can be seen, the colour intensity of the MB samples reduced with increasing treatment time. For the maximum tested treatment time of 10 minutes, a strong reduction is achieved, with only faint colouration remaining. The degradation efficiency is quantified through absorption spectroscopy. Figure 4(b) shows the degradation efficiency calculated from the measured absorbance for the MB samples of varying treatment time. As can be seen, the degradation efficiency increased significantly for small treatment times, reaching values of $\eta > 80\%$ within 3 minutes. With increasing treatment time, the degradation efficiency increases further, achieving 96% with a treatment time of 10 minutes. The achieved degradation efficiency of UoS and UICC fall within the same range, where small discrepancies are likely related to the different absorption spectroscopy system. The change in time is clearly an exponential relationship as a function of time.

3.2. Effect of air flow rate

Figure 5(a) shows the MB samples treated with varying air flow rates, ranging from 0 slpm to 3.5 slpm. An air flow rate of 0 slpm results in no generation of microbubbles and no reduction in colour intensity. Once the air flow rate is increased, a few microbubbles start generating and a reduction in colour intensity is visible. With increasing air flow rate, the colour intensity is further reduced. Figure 5(b) shows the degradation efficiency for a varying air flow rate. As can be seen, the degradation efficiency remains low at 0 slpm and jumps to $\eta > 80\%$ when microbubbles are introduced at an air flow rate of 0.5 slpm. This demonstrates that the presence of microbubbles is necessary for an effective decontamination procedure. For higher air flow rates, the number and size of generated bubbles increases, resulting in a larger absolute contact area between the plasma active species and the MB solution. The flow rate also carries additional reactive species to the treated solution volume.

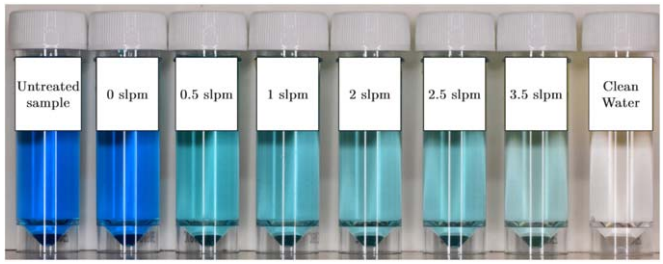

(a)

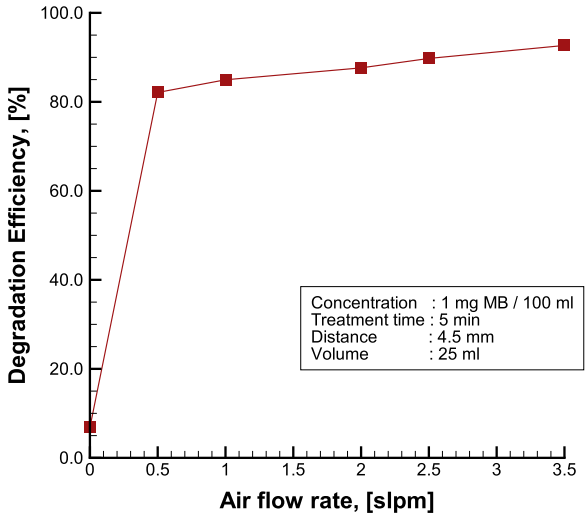

(b)

Figure 5. Effect of air flow rate on degradation efficiency.

Consequently, the degradation efficiency increases for larger air flow rates. When the air is flowing, the degradation efficiency achieves a positive linear trend with flow rate.

3.3. Effect of initial MB concentration

Figure 6(a) shows different MB samples with varying concentration ranging from 0.1 mg MB/100 ml up to 1 mg MB/100 ml before and after a 5 minutes treatment with plasma microbubbles. As can be seen, all different concentrating levels show a significant reduction in colour intensity after the treatment. Figure 6(b) shows the obtained degradation efficiency for the samples of varying initial MB concentration. The degradation efficiency holds a constant value around 90%, making the degradation efficiency independent of the MB concentration.

3.4. Effect of distance between electrode and membrane

Figure 7 shows the degradation efficiency for varying distances between the porous plasma source and the filter membrane. The two data sets are from variations using two different types of rubber gaskets with different thicknesses (0.95 mm and 1.8 mm). As can be seen, the degradation efficiency remained relatively constant with increasing distance, up to 1.1 cm. The added distance did not impact the recombination of active species before injection into the treatment solution. The ~5% reduced performance of the 1.8 mm rubber from the 0.95 mm rubber is suspected to be due to the less effective seal, allowing feed gas to inject in the water without passing through the plasma source. At small distances between electrode and membrane, the PTFE membrane can experience damage. A damaged membrane can result in a reduced performance due to a changed permeability of the membrane.

3.5. Effect of treatment volume

Figure 8 shows the degradation efficiency for varying volumes of the sample solution. As can be seen, the degradation efficiency decreased with an increasing treatment volume. A linear trend gives a decreasing 4% MB degradation efficiency per 10 ml increase of treatment solution. The linear relationship suggests that the total treated MB quantity is directly dependent upon the water volume, which directly increases the quantity of MB. So, although the degradation efficiency decreases by 14%, the total MB at that concentration increases by 333%. There is more MB being treated with increase water volume.

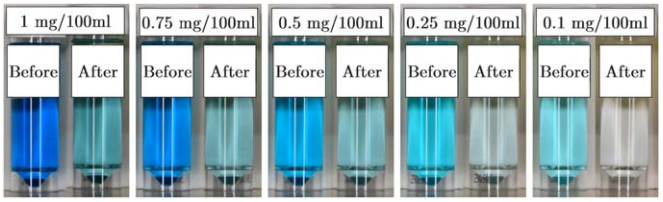

(a)

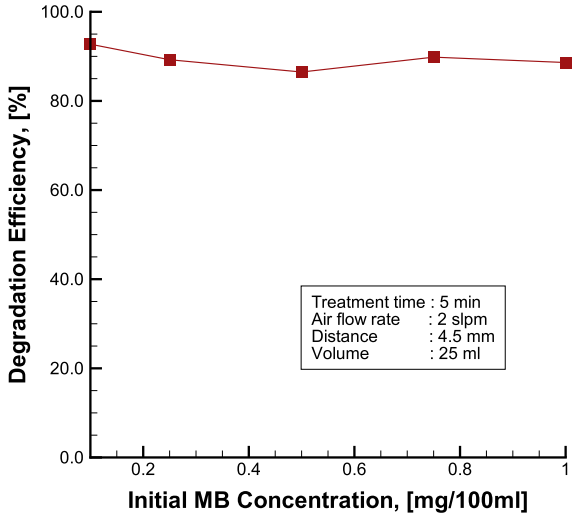

(b)

Figure 6. Effect of initial MB concentration on degradation efficiency.

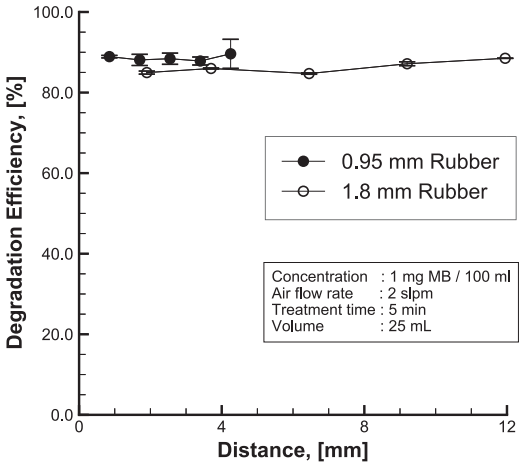

Figure 7. Effect of distance between electrode and membrane on degradation efficiency.

4. Discussion

The effects of the different parameters on degradation efficiency collectively suggest that the amount of reactive gas is the mechanism controlling the degradation rate. Both the electrode-filter distance and the MB concentration study have no noticeable impact on the degradation rate whereas the water volume and the air flow rate have linear trends. These relationships suggest that the air-water volume ratio plays a significant role in the reaction rate of the treatment process and weighted towards a larger air-water volume ratio. The yield energies from other published works supports this observation.

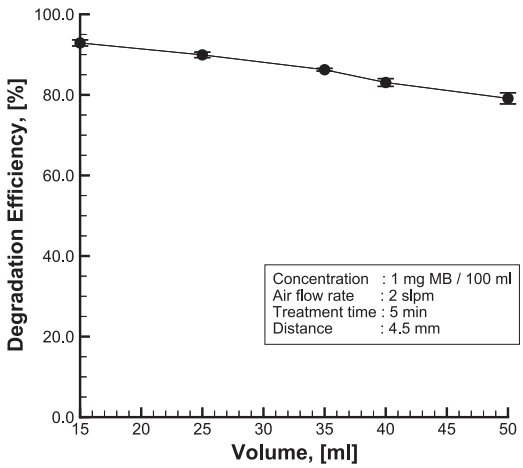

Figure 8. Effect of treatment volume on degradation efficiency.

4.1. Governing Mechanism

The lack of change to the degradation efficiency from the filter-electrode distance study, presented in figure 7, suggests that the quantity and type of reactive species entering the water volume do not change from 0.9 mm to 12 mm. The transfer time of the reactive species between the porous plasma generator and the filter membrane, with a 0.9 mm to 12 mm separation, is approximately 21 ms to 280 ms. This estimate is based on the 2 slpm flow rate and the 30 mm diameter cross-sectional area of the feed gas orifice into the water. For the air feed gas, the oxygen species involved in the degradation process are either the relatively long lived ozone, with a half-life up to a day [43] in air, or the shorter lived atomic oxygen, atomic nitrogen, and NOx species. According to a kinetic simulations by Riccardi and Barni [44] of an atmospheric DBD plasma with an electron density of 10^{21} m^{-3}, all species would recombine into primarily N_2, O_2, O_3, and N after 1 ms of leaving the discharge. All other discharge species had densities 7 orders of magnitude lower after 1 ms. The calculated transfer time of 21 ms to 280 ms between the plasma and water surface suggest that the ozone and atomic nitrogen would be the majority of the remaining reactive species present in the gas. However, concentrations of ozone and atomic nitrogen were not measured at the water surface, so the authors can only hypothesize about which reactive species play a primary role in the reaction process.

The lack of change to the degradation efficiency by the MB concentration, presented in figure 6(b), makes it appear that the concentration does not effect the reaction rate. However, it is important to recall that the degradation efficiency is normalized by the varying initial concentration for each test. So, although the initial concentration is decreasing, the final treated amount has also proportionately decreased. The trend identifies a first order exponential decay where the reaction rate is proportional to the quantity of reactants and maintains its rate constant. The reaction rate is dependent upon the concentration of the reactive species, both the MB and the reactive gas species. An increase in MB will increase the reaction rate, degrading a larger amount of MB over the same amount of time.

The flow rate parameter, presented in figure 5(b), and the water volume parameter, presented in figure 8, exhibit opposing linear trends. Both of these parameters effectively change the ratio of air to water present in the reaction, over the total treatment time. The two trends are compared in figure 9 by converting their respective dependent variables to a volume ratio of the air to water. The flow rate of the feed gas is converted to volume of air per total reaction time. The time parameter trend, presented in figure 4(b) also has its dependent variable converted to the air-water volume ratio by analyzing the 2 slpm flow rate over the treatment time at each data point. The MB concentration parameter trend, presented in figure 6(b), can be related to the air-water volume ratio by referencing both the degradation efficiency and MB concentration back to the initial 1 mg/100 ml MB concentration used by the rest of the parameter studies. The dependent variable, the degradation efficiency, is changed by normalizing the final concentration with the 1 mg/100 ml MB concentration rather than the varying initial concentration. The independent variable, the initial concentration, is converted to the air-water volume ratio by equating the change in concentration to a change in volume of the 1 mg/100 ml concentration while maintaining the same mass of MB. Although the four trend lines have different power dependencies, their trends lie along a similar linear relationship between air-water volume ratios of 300 and 700.

The consistent trend of each parameter, when converted to the air-water volume ratio, suggest that the ratio of reactive gas to MB solution is the ultimate mechanism for increasing the degradation efficiency. The total energy used to create the reactive gas remains constant, however the ratio of reactive gases to MB can be changed

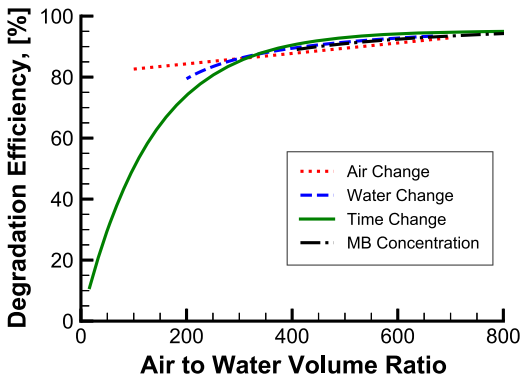

Figure 9. Effect of treatment volume, time, flow rate, and MB concentration normalized to the volume ratio of air to water.

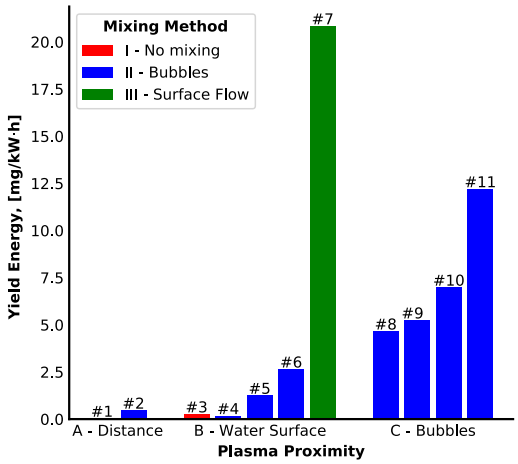

Figure 10. Yield energies reported by other authors with different MB Plasma Water Treatment configurations. Proximity of plasma to water: A—At a distance, B—At water surface, C—In bubbles. Mixing method: I—No mixing (red), II—Bubbles (blue), III—Surface flow (green). Reference association: #1 [32], #2 (This work), #3 [23], #4 [19], #5 [31], #6 [17], #7 [20], #8 [21], #9 [22], #10 [18], #11 [33].

by varying parameters which affect the quantity of reactive species: air flow rate, treated water volume, treatment time, or MB concentration. The improved degradation efficiency can therefore be explained by the relative increase in the quantity of reactive gases relative to the quantity of MB, which increases the reaction rate governed by equation (2).

4.2. Yield energy

The yield energy of this work is 0.45 g/kW·h at 25 ml of 1 mg/100 ml MB treated over 5 minutes for a 92% degradation and is shown in comparison with other works from literature in figure 10. The yield energy of 10 different MB water treatment setups from other works in literature are compared with this work in figure 10. Each value is associated with a respective reference number. Two configuration categories are also identified: 1) the proximity between the plasma discharge and the water surface (A—at a distance; B—at the water surface; and C—in bubbles) and the mixing method of the MB solution during treatment (I—no mixing (red); II—bubbles (blue); III—surface flow (green)). These two categories affect the previously discussed three mass transfer rate variables influencing the efficiency: concentration of free radicals in the gas, concentration of free radicals in the liquid, and the gas-liquid area per unit liquid volume. The proximity affects the concentration of reactive species at the gas-liquid interface. The mixing method can ensure a low concentration of reactive species in the liquid at the gas-liquid interface as wells as increasing the area per liquid volume.

The dominant treatment methods are those that produce the plasma within bubbles, where the plasma has direct contact with the water surface. In close proximity to the surface, the short-lived free radicals can directly enter the water and enhance the production of hydroxyl while reducing the energy waste from recombination, that normally occurs at a distance from the water. The one exception is #7 [20], the example of surface flow mixing, where a laminar fountain of water is exposed to a volume discharge at the water surface. For this case, the total air-water volume ratio is closer to 50% compared to bubbled systems where the gas takes up a much smaller

volume of the total reaction volume. The increased air-water volume ratio increases the interface area per liquid volume; increasing the mass transfer of reactive species, decreasing the treatment time, and reducing the total energy consumption.

Other researchers have performed reviews of plasma water treatment systems for a range of contaminants to determine the configuration characteristics that promote efficiency. Malik [45] found the configurations of the liquid for decreasing efficiency: (1) fine droplets (2) thin film (3) deep layer. Takeuchi and Yasuoka [5] found water droplets and pulsed DC discharge as the most efficient plasma treatment configuration. Magureanu *et al* [46] found that pulsed discharge and large gas-liquid surface area to be key for high efficiency.

The performance of this setup, using a bubbled surface DBD plasma system, is the fourth lowest out of the total reviewed examples, in figure 10. One reason is the proximity distance of the plasma from the water surface. As mentioned in section 4.1, although the distance between the plasma and the water can be as small as 1 mm, the performance enhancing free radicals of the plasma discharge can experience some recombination over this distance, based on the simulations by Riccardi and Barni [44]. The plasma also does not directly interact with the liquid surface, removing some of the beneficial chemical reactions [13]. Instead, the advantage of this system is its lower discharge voltage (~2 kV) due to the thin surface DBD. Although, the reduced power is not enough to compensate for the lack of direct water surface contact in the yield energy, it does reduce the power supply hardware requirements and size. The system is then more compact and portable than other plasma treatment methods, making it a viable laboratory decomposition device for contaminated solutions.

5. Conclusion

We have developed a plasma microbubble generator for the decontamination of liquids. We have quantified the performance of the plasma microbubble generator for various design and operating parameters. The feasibility study has found the treatment time to be the dominant parameter to affect the degradation efficiency, where a degradation efficiency of over 90% was achieved after a treatment time of 5 minutes. A varying initial concentration of the MB solution found no influence on the degradation efficiency, characteristic of an exponential degradation. The varying distance between the plasma source and membrane found no influence on the degradation efficiency, which suggest that the reactive gas species are those that last the 280 ms transfer time from the 12 mm distance. The varying solution volume found a linear decrease in degradation efficiency with increasing volume, but there was an overall increase to the treated MB mass, suggesting that the reaction rate increased with the increase MB in the system. The varying air flow rate found a linear increase in degradation efficiency with increased air flow, suggesting that the added reactive gases increased the reaction rate of degradation. The collection of degradation efficiency trends and review of literature yield energies suggest that a larger air-water volume ratio is the primary driving mechanism of performance, as it introduces a larger ratio of reactive gas species to MB in the reaction, increasing the reaction rate of the system. The parameter study has demonstrated the performance of the plasma microbubble generator for the decontamination of liquids. It has shown how the operating parameters of the plasma bubble reactor can be optimized to improve the MB degradation performance. The effect of the different parameters on the reaction rate has been related back to their changes to the quantity of reactants in the system.

Acknowledgments

This work is sponsored by the Defence Science and Technology LaboratoryDSTL (DSTLX-10000164754).

Data availability statement

The data generated and/or analysed during the current study are not publicly available for legal/ethical reasons but are available from the corresponding author on reasonable request.

Conflict of interest

The authors have no conflicts to disclose.

ORCID iDs

Henrike Jakob https://orcid.org/0000-0002-6035-2150

Matthew Paliwoda https://orcid.org/0000-0002-4448-6351
Minkwan Kim https://orcid.org/0000-0002-6192-312X

References

[1] USGS, Organic compounds assessed in chattahoochee river water used for public supply near atlanta, georgia, 2004 - 05, *U* (2011)
[2] Benotti M J, Trenholm R A, Vanderford B J, Holady J C, Stanford B D and Snyder S A 2009 Pharmaceuticals and endocrine disrupting compounds in u.s. drinking water *Environ. Sci. Technol.* **43** 597–603
[3] Flaws J, Damdimopoulou P, Patisaul H B, Gore A and Raetzman L 2020 Plastics, edcs & health a guide for public interest organizations and policy-makers on endocrine disrupting chemicals & plastics *Tech. Rep.*
[4] Gonsioroski A, Mourikes V E and Flaws J A 2020 Endocrine disruptors in water and their effects on the reproductive system *Int. J. Mol. Sci.* **21**
[5] Takeuchi N and Yasuoka K 2021 Review of plasma-based water treatment technologies for the decomposition of persistent organic compounds *Japan. J. Appl. Phys.* **60** SA0801
[6] U. EPA, Wastewater technology fact sheet ozone disinfection, *United States Environmental Protection Agnecy*, 1–7 (1999)
[7] Wei C, Zhang F, Hu Y, Feng C and Wu H 2017 Ozonation in water treatment: The generation, basic properties of ozone and its practical application *Rev. Chem. Eng.* **33** 49–89
[8] McClurkin J D, Maier D E and Ileleji K E 2013 Half-life time of ozone as a function of air movement and conditions in a sealed container *J. Stored Prod. Res.* **55** 41–7
[9] Loeb B L, Thompson C M, Drago J, Takahara H and Baig S 2012 Worldwide ozone capacity for treatment of drinking water and wastewater: A review *Ozone: Science and Engineering* **34** 64–77
[10] Roy A J 2010 Treatment alternatives for compliance with the stage 2d/dbpr: An economic update *Journal/American Water Works Association* **102** 44–51
[11] Mundy B *et al* 2018 A review of ozone systems costs for municipal applications. report by the municipal committee-ioa pan american group *Ozone: Science and Engineering* **40** 266–74
[12] Bruggeman P J *et al* 2016 Plasma-liquid interactions: A review and roadmap *Plasma Sources Sci. Technol.* **25** 053001
[13] Bruggeman P and Leys C 2009 Non-thermal plasmas in and in contact with liquids *J. Phys. D: Appl. Phys.* **42** 053001
[14] Parkansky N, Vegerhof A, Alterkop B A, Berkh O and Boxman R L 2012 Submerged arc breakdown of methylene blue in aqueous solutions *Plasma Chem. Plasma Process.* **32** 933–47
[15] Parkansky N, Simon E F, Alterkop B A, Boxman R L and Berkh O 2013 Decomposition of dissolved methylene blue in water using a submerged arc between titanium electrodes *Plasma Chem. Plasma Process.* **33** 907–19
[16] Luís L O, Cadorin B M, Da S Postiglione C, Postiglione S, De Souzaa I G and Debacher N A 2011 Effect of temperature on methylene blue decolorization in aqueous medium in electrical discharge plasma reactor *J. Braz. Chem. Soc.* **22** 1669–78
[17] Lee H, Yang G, Shin Y, Kim K and Hong Y C 2021 Degradation of rhodamine b and methylene blue by underwater dielectric barrier discharge *IEEE Trans. Plasma Sci.* **49** 3268–71
[18] Wu L, Xie Q, Lv Y, Zhang Z, Wu Z, Liang X, Lu M and Nie Y 2019a Degradation of methylene blue by dielectric barrier discharge plasma coupled with activated carbon supported on polyurethane foam *RSC Adv.* **9** 25967–75
[19] Wang B, Dong B, Xu M, Chi C and Wang C 2017 Degradation of methylene blue using double-chamber dielectric barrier discharge reactor under different carrier gases *Chem. Eng. Sci.* **168** 90–100
[20] Magureanu M, Piroi D, Mandache N B and Parvulescu V 2008 Decomposition of methylene blue in water using a dielectric barrier discharge: Optimization of the operating parameters *J. Appl. Phys.* **104** 103306
[21] Wu L, Xie Q, Lv Y, Wu Z, Liang X, Lu M and Nie Y 2019b Degradation of methylene blue via dielectric barrier discharge plasma treatment *Water (Switzerland)* **11** 1818
[22] Manoj Kumar Reddy P, Rama Raju B, Karuppiah J, Linga Reddy E and Subrahmanyam C 2013 Degradation and mineralization of methylene blue by dielectric barrier discharge non-thermal plasma reactor *Chem. Eng. J.* **217** 41–7
[23] Huang F, Chen L, Wang H and Yan Z 2010 Analysis of the degradation mechanism of methylene blue by atmospheric pressure dielectric barrier discharge plasma *Chem. Eng. J.* **162** 250–6
[24] Magureanu M, Bradu C, Piroi D, Mandache N B and Parvulescu V 2013 Pulsed corona discharge for degradation of methylene blue in water *Plasma Chem. Plasma Process.* **33** 51–64
[25] Jin Y, Wu Y, Cao J and Wu Y 2014 Optimizing decolorization of methylene blue and methyl orange dye by pulsed discharged plasma in water using response surface methodology *J. Taiwan Inst. Chem. Eng.* **45** 589–95
[26] Zhao Y Y, Wang T, MacGregor S J, Wilson M P, Given M J and Timoshkin V I 2014 Investigation of plasma-induced methylene blue degradation using dielectric barrier discharge *Proceedings of the 20th International Conference on Gas Discharges and their Applications* **3** 566–9
[27] Yamada M, Wahyudiono, Machmudah S, Kanda H and Goto M 2020 Nonthermal atmospheric pressure plasma for methylene blue dye decolorization by using slug flow reactor system *Plasma Chem. Plasma Process.* **40** 985–1000
[28] Krosuri A, Wu S, Bashir M A and Walquist M 2021 Efficient degradation and mineralization of methylene blue via continuous-flow electrohydraulic plasma discharge *Journal of Water Process Engineering* **40** 101926
[29] Shirafuji T and Himeno Y 2013 Generation of three-dimensionally integrated micro-solution plasma and its application to decomposition of methylene blue molecules in water *Japan. J. Appl. Phys.* **52** 11NE03
[30] Iervolino G, Vaiano V and Palma V 2019 Enhanced removal of water pollutants by dielectric barrier discharge non- thermal plasma reactor *Sep. Purif. Technol.* **215** 155–62
[31] Foster J E, Adamovsky G, Gucker S N and Blankson I M 2013 A comparative study of the time-resolved decomposition of methylene blue dye under the action of a nanosecond repetitively pulsed dbd plasma jet using liquid chromatography and spectrophotometry *IEEE Trans. Plasma Sci.* **41** 503–12
[32] García M C, Mora M, Esquivel D, Foster J E, Rodero A, Jiménez-Sanchidrián C and Romero-Salguero F J 2017 Microwave atmospheric pressure plasma jets for wastewater treatment: Degradation of methylene blue as a model dye *Chemosphere* **180** 239–46
[33] Ishijima T, Sugiura H, Saito R, Toyoda H and Sugai H 2010 Efficient production of microwave bubble plasma in water for plasma processing in liquid *Plasma Sources Sci. Technol.* **19** 1–6
[34] Suez water technologies and solutions—ozone transfer (www.suezwaterhandbook.com) accessed: 2022-11-11
[35] Lewis B W K and Whitman W G 1924 Principles of gas absorption *Ind. Eng. Chem.* **16** 1215
[36] Cheremisinoff N P and Gupta R 1983 *Handbook of Fluids in Motion* (Ann Arbor, MI, USA: Ann Arbor Science Publishers)

[37] Brandenburg R 2017 Dielectric barrier discharges: Progress on plasma sources and on the understanding of regimes and single filaments *Plasma Sources Sci. Technol.* **26** 053001
[38] Massarczyk R, Chu P, Dugger C, Elliott S, Rielage K and Xu W 2017 Paschen's law studies in cold gases *JINST* **12** 06019
[39] Muthuraman G, Teng T T, Leh C P and Norli I 2009 Extraction and recovery of methylene blue from industrial wastewater using benzoic acid as an extractant *J. Hazard. Mater.* **163** 363–9
[40] Fernandez-Perez A and Marban G 2020 Visible light spectroscopic analysis of methylene blue in water; what comes after dimer? *ACS Omega* **5** 29801–15
[41] Ball D W 2006 Field guide to spectroscopy *Field Guide to Spectroscopy* (Digital: SPIE Publications) (https://doi.org/10.1117/3.682726) 9780819478238
[42] S. Prahl, Methylene blue spectra, (1998) Accessed: 2022-12-27 (https://omlc.org/spectra/mb/)
[43] McClurkin J D and Maier D E 2010 Half-life time of ozone as a function of air conditions and movement *Julius-Kühn-Archiv* **381** 41–47
[44] Riccardi C and Barni R 2012 Chemical kinetics in air plasmas at atmospheric pressure *Chemical Kinetics* **10** 5772/38396
[45] Malik M A and Vocs D 2010 Water purification by plasmas : Which reactors are most energy efficient? *Plasma Chemistry and Plasma Processing* **30** 21–31
[46] Magureanu M, Bilea F, Bradu C and Hong D 2021 A review on non-thermal plasma treatment of water contaminated with antibiotics *J. Hazard. Mater.* **417** 125481